Pergamon

Physiology & Behavior, Vol. 56, No. 2, pp. 225–235, 1994
Copyright © 1994 Elsevier Science Ltd
Printed in the USA. All rights reserved
0031-9384/94 $6.00 + .00

0031-9384(94)E0052-6

Dissociation Between Conditioned Taste Aversion and Radial Maze Learning Following Seizure-Induced Multifocal Brain Damage: Quantitative Tests of Serial vs. Parallel Circuit Models of Memory

MICHAEL A. PERSINGER,[1] YVES R. J. BUREAU AND OKSANA PEREDERY

Behavioral Neuroscience Program, Laurentian University, Sudbury, Ontario P3E 2C6, Canada

Received 30 September 1993

PERSINGER, M. A., Y. R. J. BUREAU AND O. PEREDERY. *Dissociation between conditioned taste aversion and radial maze learning following seizure-induced multifocal brain damage: Quantitative tests of serial vs. parallel circuit models of memory.* PHYSIOL BEHAV **56**(2) 225–235, 1994.—Multivariate analyses between conditioned taste aversion (CTA) and radial maze acquisition (RMA) scores and percentages of neuronal dropout within thalamic and telencephalic structures were completed for rats in which overt seizures had been evoked following a single systemic injection of lithium/pilocarpine. Despite multifocal damage, only the amount of damage within the hippocampus (CA1) and the basolateral amygdala was most strongly associated with attenuated CTA, whereas damage within the mediodorsal thalamus was primarily associated with RMA. There was no significant correlation between CTA or RMA. Multiple regression analyses for specific Paxinos and Watson structures and their traditional aggregates supported more precise delineation of neuronal substrates of learning/memory and a multimodal (parallel) model for these processes.

Conditioned taste aversion Radial maze learning Multifocal brain damage Seizures Learning Memory

MODELS of brain function have implicitly utilized one of two dichotomous metaphors that are analogous to the fundamental spatial arrangements of electronics: series vs. parallel circuits. Elimination of one component of an aggregate of elements that is connected in series disenables the circuit and its correlative functions. Disruption of one component of an aggregate of elements that is connected in parallel does not necessarily produce any crude alteration in the output (2,10,30).

The pursuit of brain–behavioral correlates has traditionally employed the single-lesion method by which a single structure or an aggregate of spatially adjacent structures is destroyed. Either total elimination of a behavior or its converse (the occurrence of a unique behavior) is considered optimal. This bivariate approach satisfies the beliefs: 1) of scientific parsimony and 2) that the nominal presence or absence of an event is totally associated with the nominal presence or absence of a cause.

However, brain research rarely supports a strictly series model. Cohen (7) reported that destruction of all three of the separate neuroanatomical pathways that mediate learned cardioacceleration in pigeons was required before this conditioned response was eliminated. Lesions within a variety of spatially distinct brain regions usually only interfere partially with the same response. For example, intrusive (e.g., electrolytic, kainic acid injection) lesions within either the basolateral nucleus of the amygdala, insular cortices, or gustatory nuclei partially attenuate (1,8,9,18,19) conditioned taste aversion (CTA). Partial reduction of more complex behaviors such as maternal behavior (14,21) or maze learning (4,31,32) by single lesions to different single structures is also common.

These results suggest that the structural correlates of specific behaviors are arranged as multifocal aggregates that display properties of parallel circuits. However, unlike the electronic parallel circuit, the components of brain aggregates behave as modules that mediate (perhaps even qualitatively) different components to the observed behavior (2,10). This concept is particularly valid for behaviors that infer the process of memory. Its substrates are considered to be an aggregate of modules, reflecting the experience's sensory modalities, affective correlates, and previous associations (30). Indices of memory and learning are often measured artifactually as a scalar quantity for which substrates

[1] To whom requests for reprints should be addressed.

are assumed to be homogeneous and additive (i.e., increases with time or numbers of trials).

If the brain structures by which functional states (such as memory) emerge are multifocal within brain space, then the preferred method of investigation requires multiple lesions. Unfortunately, traditional (electrolysis or aspiration) and contemporary (injection of neurotoxins) techniques invariability violate the functional boundaries of the brain. What is required is a procedure that allows the brain to induce autolesions that follow intrinsic and natural pathways and structures without directly and mechanically penetrating the brain.

Honchar, Olney, and Sherman (13) first reported that injection of 3 mEq/kg of lithium chloride (LiCl) followed 24 h later by 30 mg/kg of pilocarpine induced limbic seizures that were similar to those induced by a single injection of 380–400 mg/kg of pilocarpine only (33). We (25,27) have found that injection of acepromazine within 30 min after the onset of the forepaw clonus promotes survival and is associated with remarkably consistent quantitative neuronal necrosis (17,22,25). The quantitative damage occurs within the spatial resolution that has been designated by Paxinos and Watson (20) and: 1) involves about 100 structures, 2) produces a remarkable reliability of damage within any specific structure, and 3) produces a range of cell loss between 5% and 100% between structures. Rats that have been exposed to this single treatment demonstrate permanent alterations in maternal behavior (21), radial maze learning and memory (12,25), CTA (25,34), aggression (5,25), oral dyskinesia and perseverative chewing (5), and DRL conditioning (11).

The purpose of the present study was to test the concept that two distinct types of memory—procedural or classical (CTA) vs. declarative or operant-spatial (radial arm maze)—involve parallel circuitry or a modular organization of the brain (28,30,35). Despite the large numbers of structures that were damaged, we reasoned that quantitative damage in only a small subset of these structures should be correlated with the behavioral measures that infer these memory processes. If the modular-parallel concept is correct, then: 1) more than one structure should be correlated with the behavioral measure, 2) a small number of traditional structures should produce a multiple regression equation that accommodates most of the variance in the behavioral measure, and 3) each of these measures should demonstrate relatively equal beta weights (relative contribution) to the behavioral measure.

METHOD

Subjects

A total of 33 Wistar male albino rats, obtained from Charles River Breeding facilities, served as subjects. All subjects were between 80 and 90 days of age at the time of the injection of lithium and pilocarpine. Throughout the experiment the rats were housed within temperature-regulated rooms. The LD cycle was 12:12; light onset was 0700 LT.

Procedure

Two experiments, each comprising about half the number of animals, were conducted during two summers. Eleven of the rats were injected SC with 3 mEq/kg of lithium chloride and then 4 h later with 30 mg/kg of pilocarpine; another 20 rats were injected with various combinations of one of three dosages of lithium (1, 2, or 3 mEq/kg) followed 4 or 24 h later by one of three doses (10, 20, or 30 mg/kg) of pilocarpine. Six rats received a single SC injection of 380 mg/kg of pilocarpine (33). The time between the injection and the occurrence of overt seizure activity, as defined by rearing and forelimb clonus (25), was recorded for each rat. One hour after the injection of the pilocarpine, each rat received 30 mg/kg of acepromazine; this drug was required to minimize mortality during the first 72 h (25). Rats were then returned to their home cage (three rats/cage) and administered the normal procedures (25,27) that facilitate recovery.

About 30 to 35 days after the induction of the seizures and when the rats were behaviorally recovered, they were housed singly. For each of the two experiments, half the number of rats were first given the CTA paradigm and the other half were trained in a four-arm maze. Training and testing for each procedure required about 2 weeks. After 1 week of recovery (from either the food or water deprivation), the rats were then exposed to the alternative procedure.

The CTA procedure has been described previously (26). Essentially, rats were given access to fluid for 20 min each day during the experiment. Water was given for the first 7 days. On the subsequent pairing day, rats were given access to 10% sucrose solutions and then injected IP within 1 h by 10 ml/kg of 0.15 *M* lithium chloride. After 2 days, during which time water was given during the consumptive interval, the sucrose was given once again. CTA was computed by dividing the amount of sucrose consumed (in ml) on the test day by the amount of sucrose consumed on the pairing day.

For maze training, the rats were gradually deprived of food over a 5–7-day period until they achieved 85% of their free-feeding body weight. They were then trained to press a lever for food reinforcement (50-mg Noyes pellet) for 2–3 days. Each rat was allowed to run within an automated maze for 30 min per day for 8 consecutive days. Eight sessions were considered appropriate because pilot studies demonstrated that learning asymptoted after this period.

The maze was composed of four arms, each separated by 90°, and constructed of Plexiglas. Infrared photocells along the entrance to each arm recorded entry. At the end of each maze, a standard operant lever, when pressed, delivered a 50-mg Noyes pellet by a hidden dispenser to a small food dish. To consistently obtain a reward from each arm, the rat was required to learn a pattern. It required the rat to be reinforced within each arm only once without returning (pressing the lever) in any arm until the levers in all four arms had been pressed. If the rat returned to an arm in which a reward had been obtained before activating the levers in the remaining arms, no reward was given. Total numbers of rewards and entries to each arm for each 30-min session for each rat was recorded by an IBM personal computer. Total number of successful completions was calculated by dividing the total number of rewards by four (the numbers of maze arms).

When the rats had completed both tasks, they were decapitated quickly (about 50–60 days postseizure). The brains were removed, fixed in EFA, and processed (23). A total of eight 10-μ coronal slides between the posterior and anterior commissure were stained with toluidine blue O for each rat. All of the structures, as defined by Paxinos and Watson (20), were examined at 100 and 400 × by light microscopy for damage by an experienced histomorphologist (17) who did not have access to the condition of the animal or its behavioral data. The presence or absence (0 or 1) of damage for each structure at each level was determined (22,25). The percentage of damage within the total structure was calculated by dividing the sum of the 0 and 1 scores by the number of slides in which the structure appeared, i.e., scores could range potentially between 0% and 100%.

The percentages of damage for the structures that were known (22,25) to be damaged by the lithium pilocarpine-induced seizures were loaded for each rat on a VAX 4000 computer; the CTA scores and indices of maze learning were also loaded. One-

way analyses of variance (ANOVAs) were completed between the rats that displayed the overt forelimb clonus and those that did not exhibit this behavior for all structures. One-way ANOVAs were completed between the two groups (overt seizure; no overt seizure but injected with lithium-pilocarpine). Two-way ANOVAs with one level repeated (sessions) and groups (seizured vs. nonseizured) were completed for both the numbers of circuits and their square transformations.

Multiple regressions were completed for each of the behavioral variables with only variables that met skewness criterion (i.e., ± 1.00) and with all brain variables. Considering the sample size, the maximum number of variables that were allowed to enter an equation was set equal to 4. Canonical correlation between scores for CTA and for either the raw or square root-transformed maze learning ratio and the variables that entered the multiple regression analyses for each behavioral measure were performed with and without varimax rotation; only those roots for which values were statistically significant ($p < .05$) were allowed. All analyses involved SPSS software.

RESULTS

Only 64% ($n = 21$) of the 33 rats displayed an overt seizure, as defined by rearing, forepaw clonus, and subsequent status epilepticus (before the acepromazine injection). Whereas all of the rats injected with 380 mg/kg of pilocarpine ($n = 6$) or 3 mEq/kg or lithium followed 4 h by 30 mg/kg of pilocarpine ($n = 11$) exhibited overt seizures, only 25% of the remaining rats displayed this behavior. The mean seizure onset time for the rats that displayed this response was 31 (SD, 11) min. One-way ANOVAs indicated no significant difference ($F < 1.00$) in SOT between the rats that had received the large dosage of pilocarpine or the combination of lithium and pilocarpine.

The first major effect was both qualitative and conspicuous. All rats that had exhibited overt seizures displayed significant brain damage in multiple areas (Table 1), whereas those rats that were injected with various combinations of lithium and pilocarpine and did not display overt seizures ($n = 11$) did not show any discernable brain injury. There were minimal differences in the magnitude of structural damage between the rats that were injected with only 380 mg/kg pilocarpine and 3 mEq/kg of lithium before only 30 mg/kg of pilocarpine; these results and their implications have been discussed elsewhere (6).

The means and SDs for the estimated percentage of damage within any structure (as defined by Paxinos and Watson) that exhibited discriminable neuronal dropout or gliosis are shown in Tables 1 and 2. Table 2 also shows the Spearman rho correlation coefficients between the amount of damage and the CTA or learning scores for only those structures (not included in Table 1) that exhibited a statistically significant ($p < 0.05$) association. A statistically positive correlation indicates an association between the amount of necrosis and attenuation of CTA but accelerated learning of the maze task.

One-way ANOVAs demonstrated a statistically significant [$F(1, 31) = 11.36$, $p < 0.001$; eta = 0.57] reduction in CTA for rats that displayed overt seizures (mean 0.67, SD 0.36, range 0.04–1.24), compared to the rats that did not display any seizures yet had been injected with (lower dosages of) lithium and pilocarpine (mean 0.26, SD 0.12, range 0.06–0.43). For comparison, the typical means and SDs for control rats (31) that are exposed to this paradigm have been 0.3 (0.1). Sucrose consumption during the first pairing was 25.7 (5.9) cc and 24.6 (6.3) cc for the rats that did not seizure or displayed seizures, respectively, $F(1, 31) = 0.39$, $p > 0.05$. One-way ANOVAs also indicated that rats that dissplayed necrosis also exhibited significantly [$F(1, 31) =$

TABLE 1

PERCENTAGE OF DAMAGE WITHIN DISCERNABLE STRUCTURES OF THE DIENCEPHALON AND TELENCEPHALON

Structure	Mean (SD)	Structure	Mean (SD)
ENTL	41 (31)	ENTI	31 (31)
ENTM	31 (31)	DSC	5 (15)
PAS	11 (24)	PRS	28 (20)
S	48 (36)	DG	24 (31)
CA4	30 (32)	CA2	77 (36)
CA3	67 (40)	IBL	7 (23)
OBL	4 (21)	DHC/IG	0 (0)
OC1M/B	0 (0)	OC2L/MM/ML	10 (10)
RSG	47 (27)	RSA	21 (25)
CG2	27 (33)	CG3	0 (0)
PRH	46 (31)	Te1/2/3	14 (30)
Par1/2	54 (40)	FR2	16 (24)
HL	35 (44)	FR3	22 (40)
GI	15 (22)	CLAUS	24 (36)
DI/DP/IL/LO	0 (0)	VLO/MO/VO	0 (0)
APiR	48 (33)	PIR	85 (21)
DEN	72 (30)	VEN	97 (6)
SNC/SNL	0 (0)	SNR	96 (9)
PN/STH	0 (0)	CPU	34 (19)
ASTR/FSTR	7 (20)	SSTR/PS/CB	0 (0)
EP/GP	7 (20)	ACB/SH/C	0 (0)
TU/PL/PY/PO	0 (0)	PMCO	74 (28)
PLCO	74 (25)	ACO	21 (30)
CXA	40 (35)	AHIPM	24 (25)
AHIPL	44 (40)	BLP	57 (32)
BMP	59 (34)	BLV	80 (34)
BM	38 (50)	BMA	60 (46)
LAVM	76 (24)	LAVL	86 (28)
LA	38 (50)	MEPD	16 (37)
MEPV	45 (47)	ME	19 (40)
CE(L/M/CN)	0 (0)	CE(MVP, LC, AD)	0 (0)
I	0 (0)	IM/IMG	7 (23)
AASH/AAP	4 (21)	AA	0 (0)
MGM	25 (32)	SG	53 (39)
MG	35 (48)	Reth	0 (0)
Eth	7 (23)	SC	5 (21)
Po	71 (34)	ANG	10 (30)
LPMC	50 (44)	LPLC	50 (44)
LPMR	62 (31)	LPLR	70 (37)
LDPM	79 (37)	str	0 (0)
DLG	45 (36)	VLG/PC/MC	0 (0)
IGL/SUBG	0 (0)	eml/MHB	0 (0)
LH(BL/BM/B)	10 (20)	VPM	32 (36)
VPL	42 (35)	GU	38 (50)
VM	73 (27)	VL	51 (36)
Rt	0 (0)	PV(P/A)	4 (12)
PF	71 (41)	CL	45 (38)
CM	20 (31)	PC	27 (30)
PT	55 (44)	POMN/RH	4 (10)
RE/VRE	100 (0)	G	47 (43)
im(l/vc)	0 (0)	IMD	48 (40)
MDL	81 (28)	MDPL	5 (21)
MDC	60 (41)	MDM	86 (31)
IAM	42 (50)	AM	71 (46)
AD/AV	0 (0)	AVDM	29 (46)
AVVL	21 (41)	IAD	24 (43)
BSTMA	10 (27)	LS	10 (20)

$n = 21$ brains. All other structures in telencephalon and diencephalon (including hypothalamus) not indicated are equal to 0. See index of Table abbreviations ($p < .001$).

TABLE 2

PERCENTAGE OF DAMAGE WITHIN ONLY THOSE STRUCTURES THAT WERE SIGNIFICANTLY CORRELATED WITH EITHER CTA OR MAZE LEARNING

Structure	Mean (SD)	CTA	Maze
CA1	80 (28)	0.58*	−0.30
CG1	16 (26)	−0.41*	−0.22
Par1	55 (40)	0.06	−0.48*
FR1	21 (29)	0.06	−0.37*
FL	36 (44)	−0.11	−0.44*
AI	57 (34)	0.16	−0.44*
PMCO	74 (28)	−0.44*	0.08
BLA	48 (29)	0.53*	−0.19
LADL	16 (24)	0.23	−0.40*
MEA	19 (40)	0.39*	−0.26
MGD	41 (38)	−0.44*	0.09
MGV	18 (32)	−0.45*	0.08
PIL	27 (40)	−0.37*	0.04
POT	56 (39)	−0.43*	0.27
PLI	23 (34)	−0.27	−0.36*
LDVL	77 (30)	−0.23	−0.37*
MD	55 (44)	−0.07	0.62*

n = 21 rats. *$p < .05$.

19.24, 27.68, $p < 0.001$; eta = 0.62, 0.69, respectively] lower acquisition rates [means and SDs for raw and square root = 7.6 (7.3) and 1.6 (1.3)] than the rats that did not display overt seizures or brain necrosis [raw and square root values = 71 (66) and 6.6 (3.9), respectively] yet received less concentrated injections of lithium and pilocarpine.

Figure 1 shows the mean numbers of completions of the maze during each of the eight 30-min daily sessions for the rats that either displayed or did not display the overt seizures. Multivariate analyses of variance (MANOVA), using the repeated-measures option, indicated that the rats that had initially displayed the overt seizures and brain damage (Table 1) showed fewer completions, $F(1, 31) = 17.29$, $p < 0.001$, than their cohorts. The expected learning curve was revealed in the repeated-measure (day) effect, $F(7, 217) = 60.96$, $p < 0.001$; the statistically significant group by day interaction, $F(7, 217) = 22.14$, $p < 0.001$, was due in large part to the poorer performance of the brain-damaged rats during the later sessions. Comparable effects were noted with square roots of the daily scores.

To ensure that the learning deficit was not confounded by nonspecific decreases in general ambulation, ANOVAs were completed between the mean numbers of arm entries per circuit. For the last session, the mean and SD for the numbers of entries per arm per completion were 1.1 (0.4) for the reference (nonseizure) group and 6.3 (8.5) for the brain-damaged (seizure) group [$F(1, 30) = 4.56$, $p < 0.01$; Bartlett Box = 52.85, $p < 0.001$]; the square root-transformed scores were 1.1 (0.1) and 2.1 (0.4), respectively; consequently the weaker learning rates (numbers of completions) were not an artifact of less general ambulatory activity. (Considering the disparity of variance in the numbers of entries between groups, the results indicate that some of the brain-damaged rats displayed a marked proclivity to repeatedly reenter the same arms.)

The Spearman rho correlation between numbers of entries per arm and numbers of successful completions was −0.79 ($p < 0.001$). ANOVAs for the square root of the numbers of completions after the square root of the numbers of entries (in light of the heterogeneity of variance between groups) had been covaried ($F = 26.71$, $p < 0.001$) still indicated the statistically significant group difference for that day ($F = 20.78$, $p < 0.001$ vs. $F = 35.13$, $p < 0.001$); the mean and SD for the square root of the numbers of successful completions for the group that exhibited the brain damage vs. the reference group were 3.5 (2.6) and 8.3 (1.4), respectively.

We had hypothesized that complex behaviors such as CTA or maze learning involve multiple structures (parallel processing); consequently, maximum disruption of these behaviors would require damage to multiple uncorrelated structures rather than to a single structure or its direct connection (the in series model). To test this hypothesis, multiple regression analyses were completed between the CTA score and the learning score, separately, with all structures that were damaged and (separately) with all structures for which skewness was less than the absolute value of 1.00.

The results of the multiple regressions (maximum steps set = 4) are shown in Table 3. Standardized partial regression coefficients (beta values) reflect the variables' weight for the complete equation and the percentage change in r^2 indicates the addition in explained variance as each variable entered the equation. Both the Mr and the Ar^2 (adjusted r^2) are shown; the means and SDs of the dependent are given to compare with the standard error of the estimate (SEE).

The structures that maximally predicted CTA scores varied according to the criteria of skewness. Magnitude of damage in CA1 of the hippocampus was the first and most powerful measure that predicted CTA scores when any or all structures were allowed to enter (regardless of skewness) the equation, and the amount of damage to the basolateral (anterior) nucleus of the amygdala was the most powerful predictor of CTA when the technical constraints of analyses were employed (which excluded CA1). As noted in Table 3, the four variables that entered the analyses accommodated either 70% or 86% (adjusted r^2) of the variance in CTA scores (Mr = 0.86, 0.94, respectively). The correlogram between the observed and predicted scores for CTA

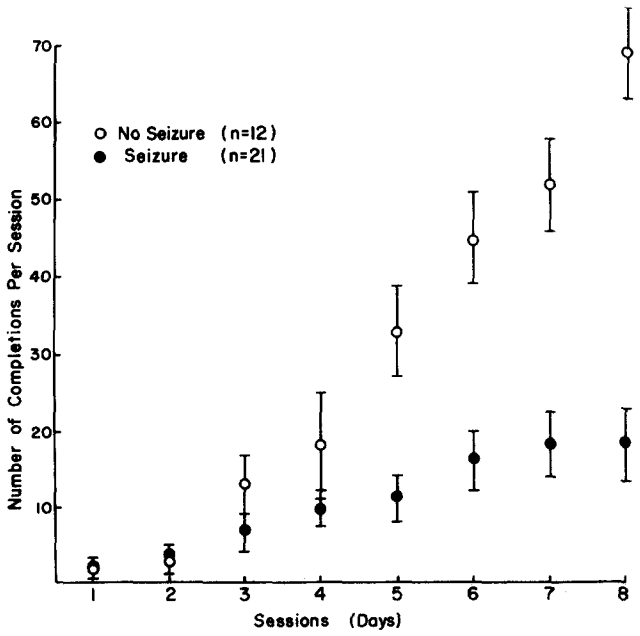

FIG. 1. Mean numbers of completions of the radial pattern per session for rats that displayed seizures (and hence brain damage) or did not display seizures after the peripheral lithium/pilocarpine injection.

values according to the equation that contained CA1 scores is shown in Fig. 2; for comparison, the mean and SD bars for CTA scores for the rats (open circle) that did not exhibit discernable brain lesions are indicated. The partial plots for each variable in the equation are shown in Fig. 3.

The four variables that maximally predicted the learning ratio accommodated between 70% and 72% of the variance in the raw or square root transformation of this measure, respectively. The same brain variables entered the equation when indices of skewness of damage were either considered or excluded. The correlogram for the equation that predicted the square root-transformed acquisition scores is shown in Fig. 4. For comparison, the mean and SD (open circle and vertical bar) for this score for the rats that did not exhibit brain injury is shown.

There was no statistically significant correlation between the equations that optimally predicted CTA and maze learning ($r < 0.10$), but strong correlations ($r > 0.90$) between the two equations that predicted CTA or the two equations that predicted learning scores. The only statistically significant correlations (Spearman rho) between any of the variables that entered the equations (Table 3) were: CA1 and BLA (0.48), POT and FL (0.45), POT and MGV (0.36), GU and PMCO (0.40), PMCO and MGV (0.42), and BLA and MGV (−0.39); Pearson r values were comparable and did not differ by more than 0.05 units.

The second hypothesis, that CTA and maze learning involve fundamentally different memory mechanisms and brain regions, was tested by canonical correlation. The two canonical covariates, CTA ratios and maze learning ratio, were analyzed as a function of the six to eight structures that entered the multiple regressions equations for both behavioral measures. Only those roots that were statistically significant beyond the $p < 0.05$ level were designated.

The correlation coefficients for each variable with each of the two significant roots and the canonical correlation coefficient associated with each root are shown in Table 4. The major structure associated with CTA scores was either BLA or CA1 and the major structure associated with maze learning was the subset of the mediodorsal complex that is designated as MD. The results were similar with both the raw and square root acquisition score. When all of the brain structures that had entered the multiple regression analyses were added as covariates, CA1, BLA, POT, and MGV loaded on the same root for CTA whereas FL and MD loaded exclusively on the root for the maze score. There were no significant differences between the two parts of the experiment for any of the above measures.

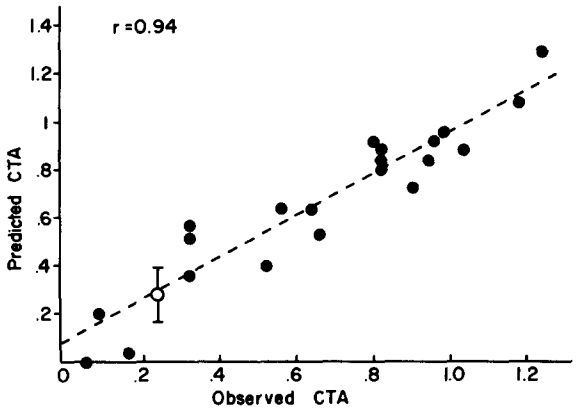

FIG. 2. Correlation between observed CTA scores and the CTA scores that were derived from the amount of damage within the key brain structures.

Subsequent Analyses

Determination or observation of an association between two phenomenon is a function of the spatial increment of analyses. Increments that are too small may be fragmental to the perception of the phenomenon whereas increments that are overinclusive may obscure phenomena. To determine if the magnitude of damage within larger increments of brain space were more conspicuously and bivariately associated with CTA and maze learning, the various structures were organized according to traditional aggregates (Table 5). Bivariate correlations between the behavioral measures and percentages of damage did not exceed 0.45, and multiple regression analyses did not produce coefficients that exceeded 0.60.

To verify that the technique by which we estimated the percentage of neuronal damage represented a reliable estimate of structural damage, we applied the principle that mean quantitative measures of a characteristic within a representative sample

TABLE 3

MULTIPLE REGRESSION VARIABLES FOR CTA AND MAZE TASKS

	CTA	CTA	Acquis	Sqrt Acquis
Variable 1	BLA	CA1	MD	MD
Beta (% chge)	0.65 (30%)	0.88 (41%)	0.44 (42%)	0.52 (38%)
Variable 2	POT	MGV	FL	FL
Beta (% chge)	−0.50 (14%)	−0.57 (32%)	−0.64 (18%)	−0.34 (17%)
Variable 3	Gu	PMCO	POT	LPMR
Beta (% chge)	−0.49 (17%)	−0.40 (10%)	0.42 (9%)	−0.36 (10%)
Variable 4	LPMR	LPLR	LPMR	AI
Beta (% chge)	0.38 (13%)	0.28 (7%)	−0.29 (8%)	−0.33 (10%)
Mr	0.86	0.94	0.88	0.87
ARSQ	0.75	0.86	0.72	0.70
SEE	0.20	0.13		0.97
Mean (SD)	0.67 (.35)	0.67 (.35)	7.6 (7.3)	1.6 (1.3)
F (all df 4, 16)	11.76	32.60	13.76	12.35

Standardized partial regression coefficients, beta; % chge = percentage change in r^2; Mr = multiple r; SEE = standard error of estimate (see text for more details).

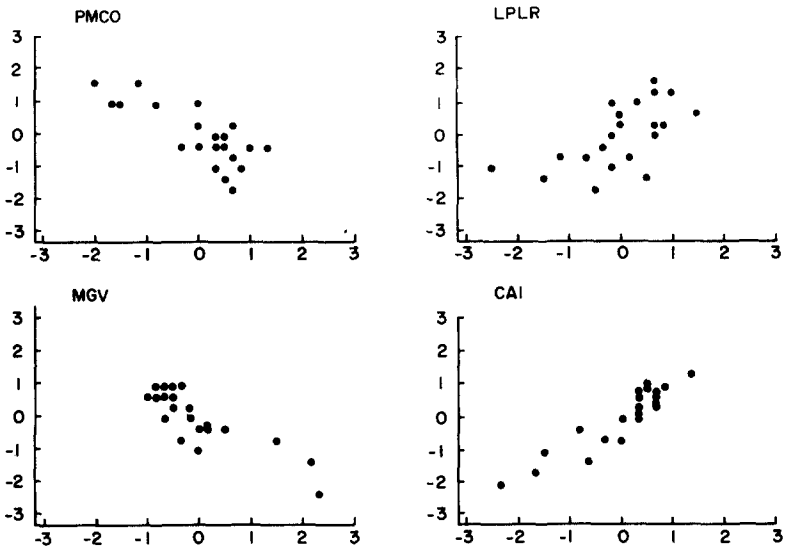

FIG. 3. Partial plots for each of the primary structures for which percentage of damage was associated with the 0.86 correlation between predicted and observed CTA.

of subsets should be concordant with the numbers of different subsets that display nominal (0 or 1) incidence of the characteristic. We applied this concept to all amygdaloid and thalamic nuclei because of the constrained spatial boundaries of these two major areas.

Consequently, individual nuclei became the cases of analyses. The average estimated percentage of the nucleus (bilaterally) that was damaged was compared with our values (obtained from other rats in another study) of the percentage of animals that displayed no damage or damage (0 or 1). As can be seen in Fig. 5, there was a strong correlation between the quantitative estimates of damage and the percentage of rats that displayed qualitative (no, yes) damage for all amygdaloid structures. Comparable strengths were evident for the thalamus.

DISCUSSION

Traditional approaches to the understanding of brain–behavioral relationships have depended primarily upon the induction of intrusive, circumscribed lesions. Although these approaches have employed a variety of methods, which have ranged from electrolytic ablation to excitotoxic necrosis, they have been structurally static and functionally inexact. In the present study, the necrotic pattern was determined naturally by the intrinsic organization of the brain and the neuropathways that were activated by the induction of limbic seizures following a single systemic injection of lithium and pilocarpine.

The results of this study both complemented and extended previous experiments. Dissociation of responses that are attributed to memories of CTA and spatial patterns of (radial maze) reinforcement following lesions of different structures was reported by Dunn and Everitt (9), who injected ibotenic acid into different brain regions. Like previous studies (9,14,17), the basolateral amygdala and the CA1 region of the hippocampus were most strongly associated with the abolition (forgetting) of CTA, whereas quantitative damage within the mediodorsal complex of the thalamus was most strongly associated with deficits in radial

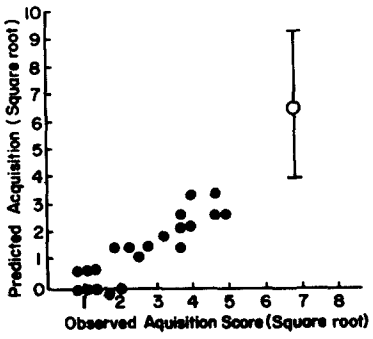

FIG. 4. Scattergram and correlation between observed acquisition scores in the radial maze and the predicted scores derived from the amount of damage within the primary structures.

TABLE 4

CANONICAL CORRELATIONS BETWEEN LEARNING/MEMORY MEASURES AND THE STATISTICALLY SIGNIFICANT BRAIN STRUCTURES (FOR BOTH BEHAVIORAL MEASURES) DETERMINED BY MULTIPLE REGRESSION

Normal Distribution			Skewed Distribution		
Variable	Root 1	Root 2	Variable	Root 1	Root 2
		Behavioral Measures			
CTA	−0.29	0.96*	CTA	0.92	0.11
Sqroot maze	0.92*	−0.42*	Sqroot maze	−0.24	0.97
		Brain Structures			
BLA	0.03	0.72*	CA1	0.67*	0.09
POT	0.33	−0.32	MGV	−0.43*	−0.15
GU	0.20	−0.26	POT	−0.44*	0.05
LPMR	−0.44*	−0.02	PMCO	−0.31	−0.12
MD	0.66*	−0.28	MD	−0.08	0.67*
FL	−0.40*	−0.36	FL	−0.07	−0.56*
AI	−0.49*	−0.01	LPLR	−0.15	−0.09
			AI	0.23	−0.43*
Can Cor coef	0.93	0.86		0.96	0.91

TABLE 5

PERCENTAGE OF DAMAGE WITHIN TRADITIONAL AGGREGATES OF STRUCTURES AND STATISTICALLY SIGNIFICANT CORRELATIONS WITH CTA AND MAZE SCORES

Structural Aggregate	Mean (SD)	CTA	Maze
Entorhinal cortex	26 (19)		
Subicular field	29 (20)		
CA fields	63 (26)		
Dentate gyrus	11 (20)		
Occipital cortex	6 (10)		
Retrosplenial cortex	35 (22)		
Cingulate cortex	14 (19)		
Temporal cortex	14 (23)		
Parietal cortex	54 (40)	NS	−0.37
Frontal cortex	26 (29)		
Insular cortex	27 (22)		
Orbital Cortex	0 (0)		
Piriform Cortex	67 (24)	NS	−0.39
Endorpiriform cortex	84 (16)		
Substantia nigra	24 (2)		
Caudate-putamen	34 (20)		
Amygdalostriatum	2 (3)		
Pallidum	4 (8)		
Ventral Striatum	2 (3)	NS	0.39
Olfactory tubercule	0 (0)		
Corticoamygdala	52 (16)		
Amygdalohippocampus	34 (28)		
Basolateral amygdala	56 (15)		
Medial amygdala	21 (14)	NS	−0.45
Central amygdala	0 (0)		
Intercalated group	4 (12)		
Anterior amygdala	4 (10)	NS	0.40
Medial geniculate	30 (20)		
Posterior thalamus	25 (13)	−0.44	NS
Lateral posterior thal	58 (25)		
Lateral dorsal thal	78 (29)		
Intermed thalamus	2 (10)		
Lateral geniculate	7 (7)		
Habenula	5 (1)		
Ventral thalamus	47 (20)		
Intralaminar thalamus	33 (14)		
Midline group thalamus	45 (8)		
Mediodorsal thalamus	42 (11)	NS	0.45
Anterior thalamus	27 (16)		
Extended Amygdala	2 (4)		
Septum	4 (5)		

n = 21 brains. All other diencephalic or telencephalic regions were not damaged.

$p < 0.05$; NS = not significant; missing values also indicate no statistically significant association.

maze learning and memory (4,28,30). Even damage within other brain regions that have been associated with place navigation (15), such as the parietal cortices (Table 1), was shown to be significantly and negatively correlated with maze acquisition in the present study.

Singular lesions, even in critical structures, usually produce only a partial deficit in the rat's ability to learn lithium chloride-induced taste aversion to sucrose. In the present study, the amount of quantitative necrosis within the basolateral (anterior part) amygdaloid nucleus was directly correlated with the attenuation of CTA. The amount of damage within the CA1 region of the hippocampus was also associated with attenuation of CTA. Total damage within either structure or partial damage that was equivalent in magnitude to damage within either structure produced a comparable magnitude in CTA reduction. The significant correlation of damage scores between these two structures is not surprising in light of these results and their reciprocal connections.

To accommodate the majority of variance in CTA scores, the amount of damage within three other structures was required. The structures that explained the largest amount of variance exhibited negative zero-order and partial-order regression coefficients; CTA intensified as the amount of damage within these structures increased. The involvement of the posterior triangularis-ventral part of the medial geniculate and the gustatory-PMCO pairs suggests the existence of inhibitory, modulating circuits that are masked by the more powerful first-order structures that mediate a significant portion of the behavior.

The likelihood that the structures that entered the equations were artifactual is minimal. The confounding role of magnitude bias (e.g., amount of damage) is unlikely because many other structures, displaying similar quantitative damage (see Tables 1 and 2), exhibited neither zero-order nor partial statistically significant correlations. A common confounding variable, the amount of generalized brain damage, was also not relevant. As noted in Fig. 2, rats that displayed damage in regions of the brain other than those involved in the explanation of the variance in CTA learned the task as well as controls. The most conspicuous argument against artifactual or spurious factors is the fact that two structures (the basolateral amygdala and CA1 hippocampus) that have been repeatedly associated with CTA were the most powerful predictors. These results reaffirm the importance of these structures, even in the presence of multifocal brain damage.

The acquisition ratio within a four-armed maze that required execution of a spatial pattern of access was also predicted most powerfully by a traditional structure: a portion of the mediodorsal thalamus. In addition, the amount of quantitative damage within the front leg portion of the frontal cortex and the agranular insular cortices also interfered with the acquisition of this task. The AI has been shown to affect radial memory during infusion of TTX (3); the inhibitory consequences of damage within the motor region of the frontal cortices that affects forelimb coordination would be expected within a maze task that requires a manipulatory response as a component of the reinforcement sequence.

There was also a novel result. The amount of damage within the MD nucleus of the mediodorsal thalamus facilitated acquisition. This result appears contradictory to previous results both

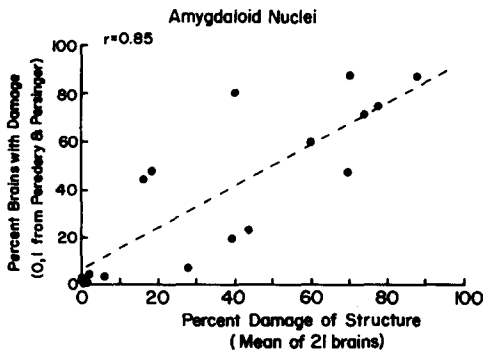

FIG. 5. Scattergram between percentage of brains that displayed either damage or no damage (20) and the percentage damage in the present study for amygdaloid nuclei in rats that were systemically injected with lithium and then pilocarpine.

from our laboratory and from the systematic work of Stokes and Best [e.g., (31)]. Although the explanation could be secondary to the differences of neuromechanisms that are elicited within Olton's radial arm maze and the automated four-arm/lever-pressing task in the present study, both procedures require retention of spatial patterns. There is also another potent explanation.

As noted in Fig. 4, the rats in which seizures had been induced and in which brain damage was quantitatively evident did not display scores that were distributed normally along the regression line (as was evident for CTA). Instead there was a conspicuous gap between the brain-damaged rats and the reference group. This suggests that all of the rats from the former group had sustained maximum brain damage within the same structures that most profoundly contribute to these behaviors. Such damage would be reflected by statistical parameters or would exhibit as maximum (mean) damage values but minimal SDs. Stated alternatively, structures with the greatest damage and lowest coefficient of variation would characterize asymptotic damage at maximum values. Considering measurement error, any structure for which damage exceeded 85% could be a candidate.

As noted in Table 1, there are several candidates that include (in decreasing order): the nucleus reuniens; the MDL and MDM; the reticula portion of the substantia nigra; the VEN; PMCO and PLCO; BLV; LAVL and LAVM. No doubt the reuniens, considering its direct input into the CA1, is a primary candidate. However, within traditional contexts, both the MDM and MLD would be classic candidates. An asymptote of damage within these two nuclei of the MD complex would explain the gap in acquisition scores between the two groups (seizure–damage; no seizure–no damage) of rats. If this conclusion is valid, then the positive association between the amount of damage within the MD portion of the MD complex and learning would suggest that this structure is normally inhibited by the MDL and MDM. There is neuroanatomical evidence for this association.

Inhibitory–excitatory equilibrium between subcomponents of traditional structures or aggregates is a common phenomenon within the nervous system. One classic example is the release of tremor by damage to a component of the extrapyramidal system that can then be eliminated or minimized by additional lesioning of a different component of that system. Disruption of all of the components of such systems is required to remove their aggregate behavioral correlates. This may explain why elimination of RAM learning required destruction of more than 85% of the MD complex; in fact, the common lesion induced by Stokes and Best (31) would have involved the MD, MDL, and MDM primarily.

The results of this study also extend previous results and emphasize the importance of utilizing intrinsic neuronal connections to mediate the brain injury. Although we found that the basolateral nucleus was the primary variable involved with CTA, only the amount of damage within the anterior portion was essential. Such specificity of subcomponents of traditional nuclear complexes within the amygdala and the thalamus could explain the inconsistences of results that are frequently seen in the literature as lesion sites became more and more circumscribed. Primary involvement of subcomponents of traditional structures also indicates that the usual perceptions of the functional spatial increments of brain space that determine behavior may be too large and overinclusive.

Table 5 shows the means and SDs for the traditional aggregates or organizations of brain structures. (For example, the basolateral amygdala would include BMP, BLA, BLV, BM, BMA, LADL, LAVM, LAVL, and LA.) Bivariate correlations between these aggregates and the behaviors were always less than 0.45 (which was not larger than the most statistically significant structure of the entire aggregate). In addition, even combinations of these variables within multiple regression equations generated coefficients that did not exceed 0.60. Such diminution of magnitude in the quantitative association between behavior and neuronal loss supports the contention that (at least in these studies) emphasis upon traditional large chunks of brain volume may dilute or mask intrinsic brain–behavioral relationships. In fact, variable or incidental overinclusion, such as during lesion studies, of adjacent structures that mediate antagonistic functions could contribute to some of the contradictions in the results between studies.

The results of the present study support the modular, parallel circuit model of memory rather than the more traditional series concept. The latter model would require total elimination of a response pattern or behavior that is associated with a complex of neuronal structures when only one component of the complex is disenabled. The numerical indicators that were used to infer the memory for both the CTA and the radial maze problem required at least four structures to explain the majority of the variance. Because the algorithms of stepwise multiple regression allows entry of variables that explain additional (rather than redundant) variance, these different structures would mediate exclusive (independent) sources of variance.

Although different structures entered in the two equations (variables were determined by a priori skewness criteria), for CTA they were intercorrelated: BLA and CA1 were significantly correlated when rank-order associations were considered; POT and MGV are spatially adjacent structures, as are LPMR and LPLR. These results suggest that the acquisition of both CTA and maze patterns involves an affective component that is mediated by the CA1–BLA–MD complex, a positional component that is mediated by the lateral posterior thalamic group, and a task-specific component. For CTA this component involves the Gu and PMCO; for the maze–lever-pressing task this component involves the forelimb portion of the frontal motor cortices.

Results of the canonical correlations verified the independence of the brain structures for which damage modified the two behavioral tasks. The statistically significant correlations between the percentage of cell loss and canonical roots involved different structures for the CTA and maze task. The complementary loading of both BLA and CA1 on the root with which CTA scores were associated reiterates the functional interaction between these structures. The significant loading of more than one structure upon the root that contains most of the variance for the maze task confirmed the results of the multiple regression analyses and indicated that, even when additional structures and behavioral measures are included in these analyses, the same primary structures emerge as specifically associated with the acquisition of this particular maze demand.

If we are to pursue the metaphor that the brain is a space–time matrix in which aggregates of elements (neuronal groups) contribute differentially to multiple domains of behaviors (25), then the utilization of techniques such as canonical correlation between sets of behavioral variables and sets of neuronal indices is essential. This approach requires: 1) measurements of responses within many different behavioral procedures for, and 2) quantification of multifocal brain damage within, the same animal. In addition to the ultimate reduction of the numbers of experimental animals that are required to study brain function, the technical procedures of multivariate analyses allow the identification of the shared sources of numerical variance within both brain structures and behavioral domains. This consequence minimizes the risk of attributing cause to a singular structure for which actual contribution to a behavior is related to a third factor: its functional role within the matrix. The employment of autolesions, such as seizure-induced damage, by which disruption

is delineated through intrinsic pathways rather than through extrinsic and arbitrary interference, should allow greater functional validity.

Despite our reliance upon numerical indicators of the percentage of neuronal dropout within multifocal regions of the rat brain, the assumption is still maintained that behavior is determined by neuronal activity and not by the absence of neurons. Cell death encourages neuroelectrical activity in associated systems that would typically have been quiescent. Dead (extirpated) zones within brain space are often surrounded by toroidal interfaces within which marked electrical lability occurs (22); this yoked spatial association could easily encourage conclusions that the extirpated region rather than the disinhibited torus of excited cells mediate the negative or positive behavioral changes. This caveat is also applicable to the present study if there is a range of quantitative cell loss that is associated with a maximum of spontaneous electrical activity within the remaining cells of the structure. As aptly stated by Solomon et al. (29) more than a decade ago, altered activity in a brain structure such as the hippocampus is more detrimental to (classical) conditioning than the removal of the structure.

ACKNOWLEDGEMENTS

Thanks to Stan Koren, Lorraine Brosseau, Christopher Blomme, and Claudette Larcher for their technical assistance.

REFERENCES

1. Aggleton, J. P.; Petrides, M.; Iversen, S. D. Differential effects of amygdaloid lesions on conditioned taste aversion learning by rats. Physiol. Behav. 27:397–400; 1981.
2. Baddeley, A. Working memory. Science 255:556–560; 1992.
3. Bermudez–Rattoni, F.; Introini–Collison, I. B.; McGaugh, J. L. Reversible inactivation of the insular cortex by tetrodotoxin produces retrograde and anterograde amnesia for inhibitory avoidance and spatial learning. Proc. Natl. Acad. Sci. USA 88:5379–5382; 1991.
4. Best, P. J.; Weldon, D. A.; Stokes, K. A. Lesions of mediodorsal thalamic nucleus cause deficits in attention to changes in environmental cues without causing sensory deficits. Ann. NY Acad. Sci. 608:705–716; 1990.
5. Bureau, Y. R. J.; Persinger, M. A. Transient blocking of persistent gnawing by haloperidol in rats with seizure-induced multifocal brain damage. Life Sci. 52:869–876; 1993.
6. Bureau, Y. R. J.; Peredery, O.; Persinger, M. A. Concordance of quantitative damage within the diencephalon and telencephalon following systemic pilocarpine (380 mg/kg) or lithium (3 mEq/kg)/pilocarpine (30 mg/kg) induced seizures. Brain Res. (in press).
7. Cohen, D. H. The neural pathways and informational flow mediating a conditioned autonomic response. In: Dicara, L. V., ed. Limbic and autonomic nervous systems research. New York: Plenum; 1974:223–275.
8. de Luca, B.; Monda, M. Neophobia, conditioned taste aversion and EEG arousal after globus pallidus lesions. Physiol. Behav. 36:545–551; 1986.
9. Dunn, L. T.; Everitt, B. J. Double dissociations of the effects of amygdala and insular cortex lesions on conditioned taste aversion, passive avoidance and neophobia in the rat using the excitotoxin ibotenic acid. Behav. Neurosci. 102:3–23; 1988.
10. Edelman, G. The remembered present: A biological theory of consciousness. New York: Basic Books; 1989.
11. Harrigan, T.; Peredery, O.; Persinger, M. A. Failure to acquire an inhibitory task following seizure-induced brain damage. Percept. Mot. Skills 70:268–270; 1990.
12. Harrigan, T.; Peredery, O.; Persinger, M. A. Radial maze learning deficits and mediodorsal thalamic damage in context of multifocal seizure-induced brain lesions. Behav. Neurosci. 105:482–486; 1991.
13. Honchar, M. P.; Olney, J. W.; Sherman, W. R. Systemic cholinergic agents induce seizures and brain damage in lithium treated rats. Science 220:323–325; 1983.
14. Insel, T. R.; Harbaugh, C. R. Lesions of the hypothalamic paraventricular nucleus disrupt the initiation of maternal behavior. Physiol. Behav. 45:1033–1041; 1989.
15. Kesner, R. P.; Berman, R. F.; Burton, B.; Hankins, W. G. Effects of electrical stimulation of amygdala upon neophobia and taste aversion. Behav. Biol. 13:349–358; 1975.
16. Kesner, R. P.; Berman, R. F.; Tardif, R. Place and taste aversion learning: Role of basal forebrain, parietal cortex and amygdala. Brain Res. Bull. 29:345–353; 1992.
17. Lafreniere, G. F.; Peredery, O.; Persinger, M. A. Progressive accumulation of large aggregates of calcium-containing polysaccharides and basophilic debris within specific thalamic nuclei after lithium/pilocarpine-induced seizures. Brain Res. Bull. 28:825–830; 1992.
18. Lasiter, P. S. Thalamocortical relations in taste aversion learning: II. Involvement of the medial ventrobasal thalamic complex in taste aversion learning. Behav. Neurosci. 99:477–495; 1985.
19. Lasiter, P. S.; Glanzman, D. L. Cortical substrates of taste aversion learning: Involvement of dorsolateral amygdaloid nuclei and temporal neocortex in taste aversion learning. Behav. Neurosci. 99:257–276; 1985.
20. Paxinos, G.; Watson, C. The rat brain in stereotaxic coordinates. Toronto: Academic Press; 1986.
21. Peredery, O.; Persinger, M. A.; Blomme, C.; Parker, G. Absence of maternal behavior in rats with lithium/pilocarpine seizure-induced brain damage: Support of MacLean's triune brain theory. Physiol. Behav. 52:665–671; 1992.
22. Peredery, O.; Persinger, M. A.; Mastrosov, L.; Parker, G. Semiquantitative patterns of lithium/pilocarpine seizure-induced damage in the rat. (submitted).
23. Persinger, M. A. Handling factors not body marking influences thalamic mast cell numbers in the preweaned albino rat. Behav. Neural Biol. 30:448–459; 1980.
24. Persinger, M. A. Personality changes following brain injury as a grief response to the loss of sense of self: Phenomenological themes as indices of local lability and neurocognitive structuring as psychotherapy. Psychol. Rep. 72:1059–1068; 1993.
25. Persinger, M. A.; Bureau, Y. R. J.; Kostakos, M.; Peredery, O.; Falter, H. Behaviors of rats with insidious, multifocal brain damage induced by seizures following single peripheral injections of lithium and pilocarpine. Physiol. Behav. 53:849–866; 1993.
26. Persinger, M. A.; Fiss, T. Mesenteric mast cell degranulation is not essential for conditioned taste aversion. Pharmacol. Biochem. Behav. 9:725–730; 1978.
27. Persinger, M. A.; Makarec, K.; Bradley, J-C. Characteristics of limbic seizures evoked by peripheral injections of lithium and pilocarpine. Physiol. Behav. 44:27–37; 1988.
28. Ross, E. D. Disorders of recent memory in humans. Trend. Neurosci. 10:170–173; 1982.
29. Solomon, P. R.; Solomon, S. D.; Vander Schaff, E.; Perry, H. E. Altered activity in the hippocampus is more detrimental to classical conditioning than removing the structure. Science 220:329–330; 1983.
30. Squire, L. R. Memory and brain. New York: Oxford; 1987.
31. Stokes, K. A.; Best, P. J. Mediodorsal thalamic lesions impair reference and working memory in rats. Physiol. Behav. 47:471–476; 1990.
32. Stokes, K. A.; Best, P. J. Mediodorsal thalamus lesions in rats impair radial-arm maze performance in a cued environment. Psychobiology 18:63–67; 1990.
33. Turski, W. A.; Cavalheiro, E. A.; Schwartz, M.; Czuczwar, S. J.; Kleinrok, Z.; Turski, L. Limbic seizures produced by pilocarpine in rats. Behavioral, electroencephalographic and neuropathological study. Behav. Brain Res. 9:315–335; 1983.
34. Venugopal, M.; Persinger, M. A.; Conditioned taste aversion in rats with a history of lithium/pilocarpine-induced limbic seizures. Neurosci. Lett. 90:177–180; 1988.

35. Wilson, F. A. W.; Scalaidhe, S. P. O.; Goldman-Rakic, P. S. Dissociation of object and spatial processing domains in primate prefrontal cortex. Science 260:1955–1958; 1993.

INDEX OF ABBREVIATIONS LISTED IN TABLE 1
(Paxinos & Watson, 1986)

Variable	Paxino and Watson's (1986) Designation
AA	anterior amygdaloid area
AAD	anterior amygdaloid area, dorsal part
AASH	anterior amygdaloid area, shell region
AAV	anterior amygdaloid area, ventral part
ACO	anterior cortical amygdaloid nucleus
AD	anterodorsal thalamic nucleus
AHIAL	amygdalohippocampal area, anterolateral part
AHIPM	amygdalohippocampal area, posteromedial part
AI	agranular insular cortex
AM	anteromedial thalamic nucleus
ANG	angular thalamic nucleus
APIR	amygdalopiriform transition area
ASTR	amygdalostriatal transition, area
AV	anteroventral thalamic nucleus
AVDM	anteroventral thalamic nucleus, dorsomedial part
AVVL	anteroventral thalamic nucleus, ventrolateral part
BLA	basolateral amygdaloid nucleus, anterior part
BLP	basolateral amygdaloid nucleus, posterior part
BLV	basolateral amygdaloid nucleus, ventral part
BM	basomedial amygdaloid nucleus
BMA	basomedial amygdaloid nucleus, anterior part
BMP	basomedial amygdaloid nucleus, posterior part
CA1	field of Ammon's horn
CA2	field of Ammon's horn
CA3	field of Ammon's horn
CA4	field of Ammon's horn
CEL	central amygdaloid nucleus, lateral division
CELC	central amygdaloid nucleus, lateral division, capsular part
CELCN	central amygdaloid nucleus, lateral division, central part
CEM	central amygdaloid nucleus, medial division
CEMAD	central amygdaloid nucleus, medial division, anterodorsal part
CEMPV	central amygdaloid nucleus, medial division, posteroventral part
CG1	cingulate cortex, area 1
CG2	cingulate cortex, area 2
CG3	cingulate cortex, area 3
CL	centrolateral thalamic nucleus
CLAUS	claustrum
CM	central medial thalamic nucleus
CPU	caudate putamen (striatum)
CXA	cortex-amygdala transition zone
DEN	dorsal endopiriform nucleus
DG	dentate gyrus
DI	dysgranular insular cortex
DLG	dorsal lateral geniculate nucleus
DSC	lamina dissecans of the entorhinal cortex
ENTI	entorhinal cortex, intermediate
ENTL	entorhinal cortex, lateral
ENTM	entorhinal cortex, medial
EML	external medullary lamina
EP	entopeduncular nucleus
ETH	ethmoid thalamic nucleus
FL	forelimb area of the cortex
FR1	frontal cortex, area 1
FR2	frontal cortex, area 2
FR3	frontal cortex, area 3
FSTR	fundus striati
G	gelatinosus thalamic nucleus
GI	granular insular cortex
GP	globus pallidus
HL	hindlimb area of the amygdala
I	intercalated nuclei of the amygdala
IAD	interanterodorsal thalamic nucleus
IAM	interanteromedial thalamic nucleus
IB1	inner blade of the dentate gyrus
IGL	intergeniculate leaf
IM	intercalated amygdaloid nucleus, main part
IMA	intramedullary thalamic area
IMD	intermediodorsal thalamic nucleus
IMG	amygdaloid intramedullary gray
IML	intermediolateral cell column
IMVC	intermedioventral thalamic commissure
INTG	intermediate geniculate nucleus
LA	lateral amygdaloid nucleus
LADL	lateral amygdaloid nucleus, dorsolateral part
LAVL	lateral amygdaloid nucleus, ventrolateral part
LAVM	lateral amygdaloid nucleus, ventromedial part
LDDM	laterodorsal thalamic nucleus, dorsomedial part
LDVL	laterodorsal thalamic nucleus, ventrolateral part
LHBL	lateral habenular nucleus, lateral part
LHBM	lateral habenular nucleus, medial part
LPLC	lateral posterior thalamic nucleus, laterocaudal part
LPLR	lateral posterior thalamic nucleus, laterorostral part
LPMC	lateral posterior thalamic nucleus, mediocaudal part
LPMR	lateral posterior thalamic nucleus, mediorostral part
MD	mediodorsal thalamic nucleus
MDC	mediodorsal thalamic nucleus, central part
MDL	mediodorsal thalamic nucleus, lateral part
MDM	mediodorsal thalamic nucleus, medial part
MDPL	mediodorsal thalamic nucleus, paralaminar part
ME	medial amygdaloid nucleus
MEA	medial amygdaloid nucleus, anterior part
MEAD	medial amygdaloid nucleus, anterodorsal part
MEAV	medial amygdaloid nucleus, anteroventral part
MEPD	medial amygdaloid nucleus, posterodorsal part
MEPV	medial amygdaloid nucleus, posteroventral part
MG	medial geniculate nucleus
MGD	medial geniculate nucleus, dorsal part
MGM	medial geniculate nucleus, medial part
MGV	medial geniculate nucleus, ventral part
MHB	Medial habenular nucleus
OC1M	occipital cortex, area 1, monocular part (primary visual cortex)
OC2L	occipital cortex, area 2, lateral part
OC2ML	occipital cortex, area 2, mediolateral part
OC2MM	occipital cortex, area 2, mediomedial part
PAR1	parietal cortex, area 1
PAR2	parietal cortex, area 2
PAS	parasubiculum
PC	paracentral thalamic nucleus
PF	parafascicular thalamic nucleus
PIL	posterior intralaminar thalamic nucleus
PIR	piriform cortex
PLD	paralambdoid septal nucleus
PLI	posterior limitans thalamic nucleus
PLCO	posterolateral cortical amygdaloid nucleus
PMCO	posteromedial cortical amygdaloid nucleus
PO	posterior thalamic nuclear group
POMN	posteromedian thalamic nucleus

POT	posterior thalamic nuclear group, triangular group
PRH	perirhinal cortex
PRS	presubiculum
PT	paratenial thalamic nucleus
PV	paraventricular thalamic nucleus
PVA	paraventricular thalamic nucleus, anterior part
PVP	paraventricular thalamic nucleus, posterior part
RE	reuniens thalamic nucleus
RETH	retroethmoid nucleus
RH	rhomboid thalamic nucleus
RSA	retrosplenial agranular cortex
RSG	retrosplenial granular cortex
RT	reticular thalamic nucleus
S	subiculum
SG	suprageniculate thalamic nucleus
SNC	substantia nigra, compact part
SNL	substantia nigra, lateral part
SNR	substantia nigra, reticular part
SPFPC	subparafascicular thalamic nucleus, parvocellular part
STR	superior thalamic radiation
SUBG	subgeniculate nucleus
TE1	temporal cortex, area 1 (primary auditory cortex)
TE2	temporal cortex, area 2
TE3	temporal cortex, area 3
VEN	ventral endopiriform nucleus
VL	ventrolateral thalamic nucleus
VLG	ventral lateral geniculate nucleus
VLGMC	ventral lateral geniculate nucleus, magnocellular part
VLGPC	ventral lateral geniculate nucleus, parvocellular part
VM	ventromedial thalamic nucleus
VP	ventral pallidum
VPL	ventral posterolateral thalamic nucleus
VPM	ventral posteromedial thalamic nucleus
VRE	ventral reuniens thalamic nucleus